International Journal of Multidisciplinary Research and Growth Evaluation.

Study of dust properties nearby pulsar J0302+2252 using Iris, Akari and wise surveys

Kushal Khatiwada [1], Keshab Chaudhary [2], Anil Subedi [3], Ramchandra Kandel [4], Ashok Chaudhary [5], Devendra Raj Upadhyay [6], Ajay Kumar Jha [7*]

[1, 3, 4, 6] Department of Physics, Amrit Campus, Tribhuvan University, Kathmandu, Nepal

[2, 5, 7] Central Department of Physics, Tribhuvan University, Kathmandu, Nepal

* Corresponding Author: **Ajay Kumar Jha**

Article Info

ISSN (online): 2582-7138
Volume: 04
Issue: 02
March-April 2023
Received: 08-02-2022;
Accepted: 02-03-2022
Page No: 131-136

Abstract

A search of dust structures nearby the pulsar J0302+2252 in IRIS, AKARI, and WISE surveys were performed using Skyview Observatory (http://skyview.gsfc.nasa.gov). The physical properties have been studied at 60µm & 100µm in the IRIS survey, 90µm & 140µm in the AKARI survey, and 12µm & 22µm in the WISE survey at right ascension (R.A.) (J2000)=03^h 02^m 31.99^s and Declination (Decl.) (J2000)=+ 22^0 52^m 12.10^s . In this work, we have studied the physical properties such as Dust color temperature, Planck's function, Visual extinction, and Mass profile of the dust using the data reduction software ALADIN v11. The dust color temperature is found to be 22.271 ± 0.261K in IRIS, 22.343 ± 0.939 K in AKARI, and 278.74 ± 0.067 K in WISE. Also, the dust mass is found to be 2.286×10^{27} kg (1.149×10^{-3} M⊙) in IRIS, 8.800×10^{26} kg (0.416×10^{-3} M⊙) in AKARI and 5.220×10^{25} kg (0.026×10^{-3} M⊙) in WISE. The average visual extinction is found to be 1.372×10^{-13} mag. In IRIS, 4.970×10^{-14} mag. In AKARI and 1.673×10^{-15} mag. In WISE. The dust color temperature and dust mass distribution show a very good agreement with Gaussian. The Contour plots of dust color temperature and dust mass show inverse relation between them in all three bands IRIS, AKARI, and WISE.

DOI: https://doi.org/10.54660/.IJMRGE.2023.4.2.131-136

Keywords: ISM, IRIS, Dust color temperature; Dust mass

Introduction

The interstellar medium (ISM) of the galaxy has a complicated distribution of cavities, filaments, arcs, loops, lobes, and shells [1]. When large stars (8–25 M⊙) go supernova, they leave behind neutron stars that are rapidly revolving. To put it another way, a large star undergoes a supernova explosion and the star's core collapses to produce a neutron star. Its surrounding materials, or stellar debris, accelerate their departure. On the other hand, this event has enriched the interstellar medium (ISM) with material heavier than hydrogen and helium, which not only causes a disruption in the ISM but also causes it to become disturbed [2].

Studying the distribution of star-forming materials in molecular clouds is essential to comprehending how they develop and ultimately give rise to stars [3]. The argument for neutron stars being the cause of the recently found pulsating radio emissions [4]. A neutron star is formed by collapsing the center of a star by a massive explosion of a supernova, the charge of the neutron star moves with a speed nearly the speed of light due to its magnetic and spinning axis of radio wave being generated [5]. A rotating neutron star having a strong magnetic field nearly in dipolar form is called a pulsar [6]. Pulsars are unusually rotating strongly magnetized neutron stars that generate strength emissions by exploiting the lack of rotational kinetic strength [4]. The pulse period of known pulsars ranges from 1.5ms to 11 seconds [7]. The majority of pulsars can only be observed at radio wavelengths, but roughly 30 of them, mostly young and short-period pulsars, can also be observed at the optical, x-ray, and even gamma-ray wavelengths. About half of these can only be observed at high energies [8]. The pulsar is mainly observed in the galactic plane in supernova remnants [9].

Jha *et al*. (2018) studied far infrared (60 µm and 100 µm) IRAS loop at -5° Galactic latitude around pulsar J1627-5547 by taking different dust properties like Dust Color Temperature, Dust Mass, and Inclination angle and they conclude that the results are agreed with Gaussian similar works are also done by Chaudhary *et al*. (2022). Several research has been performed exploring the properties of interstellar dust using the infrared data in the region near the Pulsars [10,11], White Dwarfs [12,13], AGB Star [14,15], Supernova Remnants [16], FIR loops [17, 18], FIR Cavities [19], etc., using the data from IRAS, IRIS, and AKARI. In this work, we have studied the multiwavelength variation of dust color temperature together with dust mass near the pulsar J0302+2252 using IRIS, AKARI, and WISE surveys.
This work intends to explore the information about the formation and the different dust properties like dust mass and dust temperature properties that helps to better ways to understand the stars and different galaxies.

2. Materials and method

The source name, right ascension, declination, and other characteristics were obtained via the ATNF pulsar catalog(https://www.atnf.csiro.au/research/pulsar/psrcat/) source coordinates were found using SIMBAD(https://simbad.u-strasbg.fr/simbad/sim-fid) and Sky View Virtual Observatory (https://skyview.gsfc.nasa.gov/current/cgi/titlepage.pl) used those coordinates as input. We have downloaded our candidate's JPEG and FITS images at several wavelengths, such as 12μm and 24μm in WISE, 60μm and 100μm in IRIS, and 90μm and 140μm in AKARI. Aladin V2.5 and V11.5 were used to examine each pixel of the FITS images. After obtaining the flux value for each pixel in the FITS image, further calculations were done.

2.1 Dust Temperature

We have used the method of Dupac *et al*. and Schnee *et al*. to calculate the dust color temperature [20, 21].

For IRIS

The expression to calculate the dust color temperature for IRIS survey is:

$$T_d = \frac{-96}{\ln\left[R \times 0.6^{3+\beta}\right]} \quad (1)$$

Where, flux density ratio, R, is given by:

$$R = \frac{F(60\mu m)}{F(100\mu m)} \quad (2)$$

The F(60µm) & F(100µm) are the value of flux densities at 60 & 100 microns, respectively. The spectral emissivity index value, β, is determined by dust particle parameters such as composition, size, and compaction. A pure black substance has a value of β =0, amorphous layer lattice matter has a value of β =1, and crystalline dielectric has a value of β =2

For AKARI

The expression for dust color temperature in the AKARI survey is:

$$T_d = \frac{-57}{\ln\left[R \times 0.64^{3+\beta}\right]} \quad (3)$$

Where, flux density ratio, R, is

$$R = \frac{F(60\mu m)}{F(140\mu m)} \quad (4)$$

Here, F(90µm) and F(140µm) are the flux densities at 90 µm and 140 µm respectively.

For WISE

The expression for dust color temperature in the WISE survey is:

$$T_d = \frac{-546}{\ln\left[R \times 0.54^{3+\beta}\right]} \quad (5)$$

Where, flux density ratio, R, is

$$R = \frac{F(12\mu m)}{F(22\mu m)} \quad (6)$$

2.2 Planck's Function

The Planck's function is a well-known function [20], given by the equation,

$$B(\upsilon, T_d) = \frac{2h\upsilon^3}{c^2}\left[\frac{1}{e^{\left(\frac{h\upsilon}{K_B T_d}\right)}-1}\right] \quad (7)$$

Where,
h = Planck's constant,
ν = frequency with which radiation is observed, and
T_d = average temperature of the region
c = speed of light.

2.3 Mass of Dust

The dust mass is estimated using the Infrared flux density. The thus resulting value of the dust mass is based on the chemical and physical characteristics of the particle, the temperature of the dust (Td) and the distance between the object and the observer (D) [21]. To calculate the mass of the dust first, the flux density is given by;

$$F_\nu = NB(\nu, T_d)Q(\nu)^{\frac{\pi a^2}{D^2}} \quad (8)$$

Where Q(ν) is the dust particle emissivity index. The dust mass is calculated as;

$$M_d = \frac{4\alpha\rho}{3Q(\upsilon)}\frac{F(\upsilon)D^2}{B(\upsilon, T_d)} \quad (9)$$

Here,
α = weighted dust particle size,
ρ = dust particle density, Q_υ=dust particle emissivity
$F\upsilon$ =f ×MJy/sr ×5.288× 10^{-9}, where MJy/sr = 1× 10^{-20} kg s^{-2} and f = measured relative flux density from the image.

3 Results and Discussion

3.1 A linear Fitting of Flux

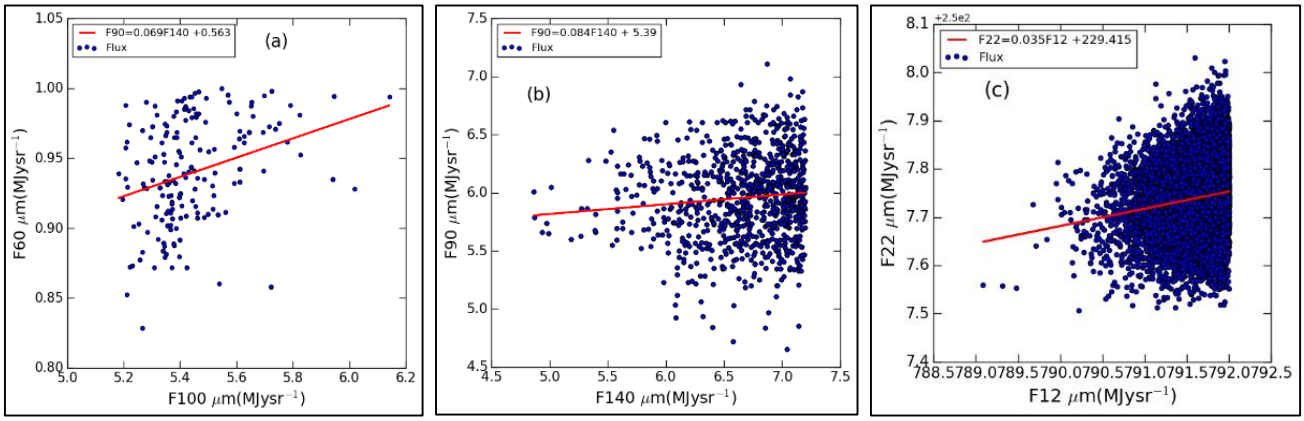

Fig 1: Scatter plots with linear best fit (a) IRIS: F100 µm vs F60 µm, (b) AKARI: F140 µm vs 90 µm, and (c) WISE: F12 µm vs F22 µm. The dots indicate the flux, whereas the straight line provides the best-fit line.

A best-fit line between IRIS F100 µm and F60 µm, AKARI F140 µm and F90µm, and WISE F12 µm and F22 µm along the X-axis and Y-axis, respectively, represents the flux distribution in Figure 2 (a), (b), and (c). The greatest flux density zone is used to depict the most occupied area. In the context of AKARI, the flux is linearly distributed, and the slope, intercept and correlation coefficient (r) are all calculated to be 0.840, 5396 and 0.099. Similarly, in the IRIS and WISE, the flux is linearly distributed, and the slope and correlation coefficient (r) are all calculated to be 0.069, 0.295, and 0.035, 0.160 respectively.

3.2 Distribution of Dust Temperature

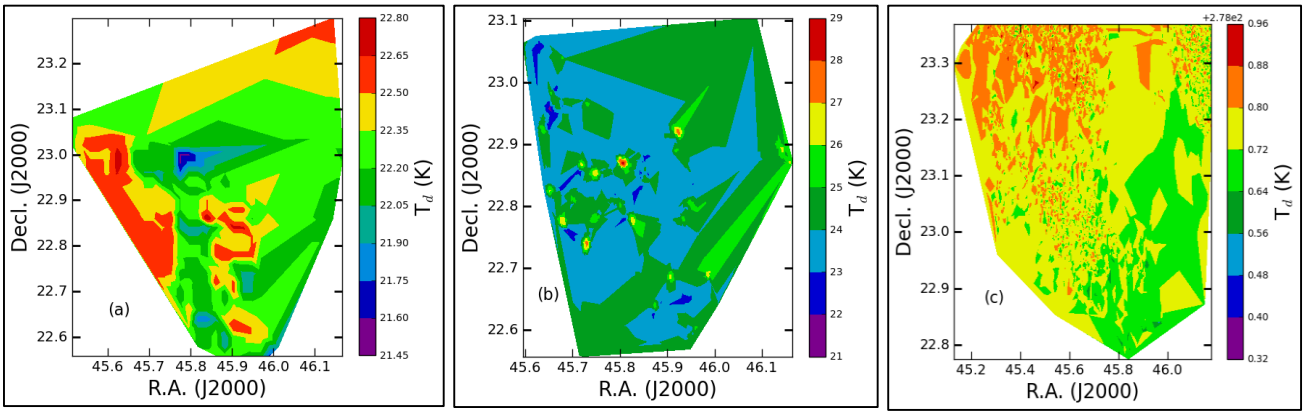

Fig 2: The contour plot of (a) IRIS: R.A. versus Decl. versus Temperature (b) AKARI: R.A. versus Decl. versus Temperature (c) WISE: R.A. versus Decl. versus Temperature at R.A.= $03^h\ 02^m\ 31.99^s$, Decl. =$+20^o\ 52^m\ 12.10^s$.

The contour map of temperature fluctuation from the IRIS, AKARI, and WISE surveys is shown in Figure 3(a), (b), and (c). The IRIS survey determined that the maximum temperature of 22.568 ±0.216 K in some areas of the outside region and a minimum of 21.702±0.216 K in areas closer to the core. Similar to this, in the AKARI survey was found to be 24.466 ±0.939K with maximum temperature of 24.343±0.939K in the centre and the maximum and minimum temperatures for WISE are found to be 278.769 K ± 0.067 K and 278.630 K ± 0.067 K respectively. The minimum temperature region indicates the region having cold ISM matter, and the maximum temperature region indicates the region having warm ISM matter.

3.3 Distribution of Dust Mass

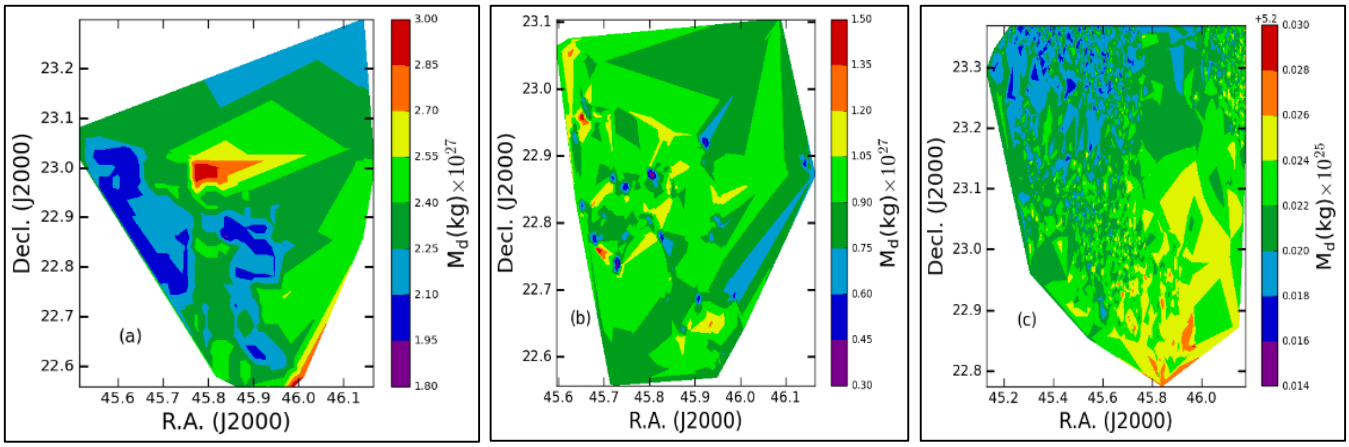

Fig 3: The contour plot of (a) IRIS: R.A. versus Decl. Versus Dust Mass (b) AKARI: R.A. versus Decl. Versus Dust Mass (c) WISE: R.A. versus Decl. Versus Dust Mass at R.A. =$03^h\ 02^m\ 31.99^s$,Decl.= $+22^o\ 52^m\ 12.10^s$.

The contour map of the dust mass variation is shown in the figure 4 (a) IRIS (b) AKARI and (c) WISE surveys. The colour bar indicates that the distribution of mass is greatest in the core region and least in the outer region in all three surveys. In the IRIS survey, the maximum mass and minimum mass was found to be 2.987×10^{27}kg and 2.097×10^{27} kg respectively. Likewise, the maximum and minimum mass in AKARI survey was found to be 8.461×10^{26} Kg and 8.224×10^{26} kg respectively. In WISE, the maximum and minimum value of dust mass was found to be 5.227×10^{25} kg and 5.219×10^{25} Kg respectively.

3.4 Normal with Histogram Plot of Temperature

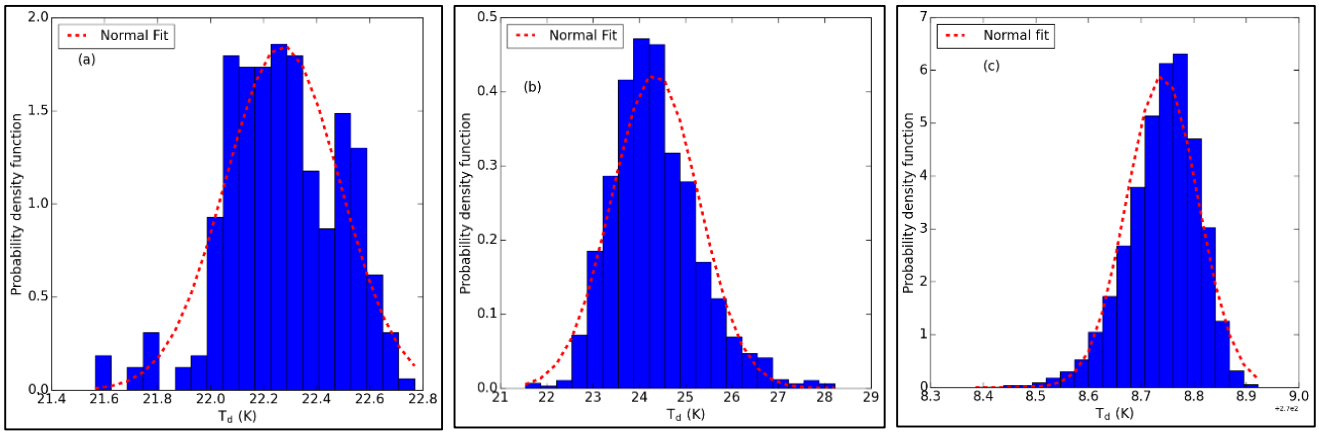

Fig 4: Normal with histogram plot of (a) Temperature versus probability density function: IRIS (b) Temperature versus probability density function: AKARI and (c) Temperature versus probability density function: WISE. The graph between the temperature and probability density function is slightly skewed to the left side in IRIS and WISE and normally distributed in AKARI.

The normal plot with the histogram of temperature versus probability density function is shown in Fig. (5) (a), (b), and (c). The curve is slightly skewed to the right in IRIS and AKARI surveys and normally distributed in the wise survey. The normal center is found to be 22.271 K in IRIS, 24.343 K in AKARI, and 278.740 K in WISE.

3.5 Normal with the Histogram Plot of Mass

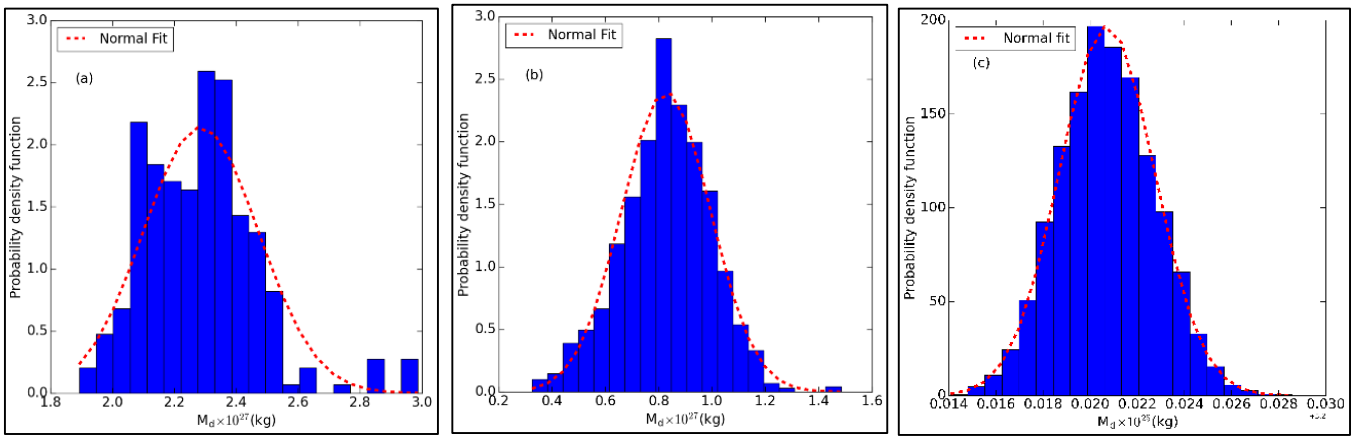

Fig 5: Normal with histogram plot of (a) Mass versus probability density function: IRIS (b) Mass versus probability density function: AKARI and (c) Mass versus probability density function: WISE

Fig. (5) (a), (b), and (c) are the normal distribution with the histogram plot of dust Mass in IRIS, AKARI and WISE surveys respectively. The normal centre is found to be 2.286 $\times 10^{27}$ kg in IRIS, 0.828×10^{27} kg in AKARI and 5.220 $\times 10^{25}$ kg in WISE survey.

4 Conclusion

The main aim of our study is to find the physical properties of dust nearby pulsar J0302+2252 such as dust mass , dust color temperature and plank's function and their relation around it. These are the conclusion that can be drawn from our study.

- The dust color temperature is found in the range between 21.702 K ± 0.216 K to 22.568 K ± 0.216 K in the IRIS survey, 24.342 K ± 0.939 K to 24.466 K ± 0.939 K in AKARI survey and 278.630 K ± 0.067 K to 278.769 K ± 0.067 K in WISE survey.
- The minimum and maximum dust mass is found to be 2.097×10^{27} kg (1.053×10^{-3} M⊙) and 2.987×10^{27} kg (1.501×10^{-3} M⊙)in IRIS , 8.224×10^{26} kg (0.413×10^{-3} M⊙ and 8.461×10^{26} kg (0.425×10^{-3} M⊙) in AKARI and 5.219×10^{25} kg (2.622×10^{-5} M⊙)and 5.227×10^{25} kg (2.627×10^{-5} M⊙) in the WISE survey.
- The average dust color temperature was found to be 22.271 K in IRIS, 24.343 K in AKARI, and 278.740 K in the WISE survey. The dust color temperature is higher in WISE as it has an inverse relation with wavelength.
- The dust color temperature and the dust mass are inversely proportional to each other.
- The average visual extinction is found to be 1.372×10^{-13} mag. in IRIS, 4.970×10^{-14} mag. in AKARI and 1.673 × 10-15 mag. in WISE. The inverse relation between extinction and temperature is described as the correlation coefficient value is found to be negative and low values suggest oscillating nature to get powerful equilibrium.

5 Acknowledgements

We are grateful to the Department of Physics, Amrit Campus, and the Central Department of Physics, Tribhuvan University for giving us the opportunity to work in this scientific field. This study made use of the Gaia Archive, SIMBAD data base, SkyView Virtual Observatory, IRIS survey, AKARI survey, and WISE survey.
One of the authors (Kushal Khatiwada) acknowledges UGC, Nepal for this research support.

References

1. Jha AK, Aryal B. A study of far infrared loop at-5o Galactic latitude around pulsar J1627-5547. BIBECHANA. 2018; 15:70. (https://doi.org/10.3126/bibechana.v15i0.18443)
2. Jha AK, Aryal B. A study of a cavity nearby a pulsar at-60º latitude in the far infrared map. Journal of Nepal Physical Society. 2017; 4(1):33. (https://doi.org/10.3126/jnphyssoc.v4i1.17334).
3. Arce HG, Goodman AA. An extinction study of the Taurus dark cloud complex. The Astrophysical Journal. 1999; 517(1):264.
4. Gold T. Rotating neutron stars as the origin of the pulsating radio sources. Nature. 1968; 218(5143):731. (10.1038/218731a0).
5. Jha AK, Aryal B. A study of a pulsar wind driven structure in far-infrared Iras map at lattitude-10º. Journal of Institute of Science and Technology. 2017; 22(1):1-9. (https://doi.org/10.3126/jist.v22i1.17733).
6. Sturrock PA. A model of pulsars. The Astrophysical Journal. 1971; 164:529.
7. Lattimer JM, Prakash M. The physics of neutron stars. Science. 2004; 304(5670):536. (10.1126/science.1090720).
8. Thompson C, Duncan RC. The soft gamma repeaters as very strongly magnetized neutron stars. II. Quiescent neutrino, X-ray, and Alfven wave emission. The Astrophysical Journal. 1996; 473(1):322.
9. Ostriker JP, Gunn JE. On the nature of pulsars. I. Theory. The Astrophysical Journal. 1969; 157:1395. (https://doi.org/10.1086/150160).
10. Joshi IN, Jha AK, Aryal B. A study of dust structure nearby white dwarf WD1334-678. Bibechana. 2021; 18(2):130. https://doi.org/10.3126/bibechana.v18i2.37439.
11. Paudel MS, Bhandari P, Bhattarai S. Study of Dust Cavity around the White Dwarf WD 0352-049 in Infrared Astronomical Satellite Map. Journal of Nepal Physical Society. 2021; 7(2):110. https://doi.org/10.3126/jnphyssoc.v7i2.38631.
12. Jha AK, Upadhyay DR. Dust Structure around two Asymptotic Giant Stars at Latitude 32° &

40.67°. Himalayan Physics. 2017; 6(7):41. https://doi.org/10.3126/hj.v6i0.18356.
13. Gautam SP, Silwal A, Tiwari M, Subedi S, Khanal M, Jha AK. Dust Properties of Two New Cavity Structures Nearby Asymptotic Giant Branch Stars: The IRAS Survey. Journal of Institute of Science and Technology. 2021; 26(2):119. https://doi.org/10.3126/jist.v26i2.41556.
14. Jha AK, Yadav A, Upadhyay DR, Aryal B. Dust Properties of Super-Nova Remnant (Crab Nebula) Using AKARI Survey. Journal of Nepal Physical Society. 2021; 7(4):64-70. https://doi.org/10.3126/jnphyssoc.v7i4.42933.
15. Jha AK, Aryal B, Weinberger R. A study of dust color temperature and dust mass distributions of four far infrared loops. Revista mexicana de astronomía y astrofísica, 2017, 53(2). http://www.scielo.org.mx/scielo.php?script=sci_arttext&pid=S0185-11012017000200019
16. Jha AK, Aryal B. Dust color temperature distribution of two FIR cavities at IRIS and AKARI maps. Journal of Astrophysics and Astronomy. 2018; 39(2):1-7. https://doi.org/10.1007/s12036-018-9517-6.
17. Tiwari M, Gautam SP, Silwal A, Subedi S, Paudel A, Jha AK. Study of Dust Properties of two Far Infrared Cavities nearby Asymptotic Giant Branch stars under Infrared Astronomical Satellite Maps. Himalayan Physics. 2020; 9:60. https://doi.org/10.3126/hp.v9i01.40193.
18. Chaudhary A, Thapa B, Sodari T, Chaudhary K, Upadhyay DR. Distribution of Dust Color Temperature, Planck's Function, and Dust Mass around PSR J1240-4124. Journal of Nepal Physical Society. 2022; 8(1):88. (https://doi.org/10.3126/jnphyssoc.v8i1.48292).
19. Gautam SP, Silwal A, Jha AK. Dust color temperature and Planck function distribution of a far infrared planetary nebula at 90 and 140 μm AKARI map. International Astronomy and Astrophysics Research Journal, 2020, 1. (http://sciarchives.uk/id/eprint/161).
20. Schnee SL, Ridge NA, Goodman AA, Li JG. A complete look at the use of IRAS emission maps to estimate extinction and dust temperature. The Astrophysical Journal. 2005; 634(1):442. (10.1086/491729).
21. Dupac X, Bernard JP, Boudet N, Giard M, Lamarre JM, Mény C, *et al*. Inverse temperature dependence of the dust sub millimetre spectral index. Astronomy & Astrophysics. 2003; 404(1):L11. (10.1051/0004-6361:20030575).